A Grid-Based Coverage Analysis of Urban mmWave Vehicular Ad Hoc Networks

Mumin Ozpolat, Erik Kampert, Paul A. Jennings, Matthew D. Higgins, *Senior Member, IEEE*

***Abstract*—In this letter, a tractable coverage model, specifically designed for urban vehicular *ad hoc* networks, is presented to aid a better system designer. This is achieved through the use of a model based upon line processes, which simplifies the analysis. It is found, that even in crowded interferer scenarios, mmWave vehicular communications can establish reliable links with an SINR threshold of around 5 dB, with a coverage probability of approximately 0.8 at 50 m separation between a *typical* transmitter and a *typical* receiver. These results, and their inference towards the design and deployment of urban vehicular ad-hoc networks, may impact the developments of future vehicle-to-vehicle (V2V) applications and services.**

***Index Terms*—mmWave, Vehicular Ad Hoc Networks, Stochastic Geometry, Blockage Effect, Poisson Point Process (PPP)**

I. Introduction

THE millimeter wave (mmWave) communications channel, alongside massive multiple-input and multiple-output (MIMO) methods, are seen to be core pillars of gigabit-per-second connectivity between vehicles [1][2]. To solve challenges in analyzing the performance of such connectivity, stochastic geometry is a common mathematical toolset employed. The stochastic mathematical modeling of vehicular communications using the mmWave channel presents many challenges, which, amongst others, include accurately representing the distribution of vehicles, their beam widths, and their line-of-sight (LOS) and non-line-of-sight (NLOS) statistics. Thus, a tractable mathematical coverage model that takes into account all these challenges is an ambition in the community. The blockage model of the vehicular environment that is presented in this Letter, provides an enhanced representation of the grid-like distribution of vehicles. By taking into account the directionality of beams through massive MIMO, this leads to an improved analysis of the coverage performance of mmWave vehicular communications. A brief comparison between mmWave vehicular communications and Vehicular Ad Hoc Networks (VANET) is presented for completeness.

A. Related Work

Intuitively, urban *ad hoc* vehicular communications networks can only exist within the bounded urban corridors formed along the roads by buildings, foliage etc. Empirical evidence for the strong influence of the urban corridor on the coverage of the transmitter has been provided by measurements in [3], performed at a carrier frequency of 55 GHz and involving a transmitter antenna with a 10° beam width installed on the top of a building and a mobile receiver vehicle with a 20° beam width. Strong signal propagation is limited to the street in which the transmitter is installed and the streets at right angles to this street, whereas propagation at parallel streets is negligible.

Another important aspect of mmWave V2V communications modelling is the NLOS effect of obstructing vehicles between the *typical* transmitter and receiver. For instance, [4] has modelled large vehicles as blockage for highway mmWave V2I communications. As presented in [5], measurements carried out at a carrier frequency of 77 GHz indicate that an obstructing vehicle has a negligible effect on V2V communications, because the gap between the vehicle's under-body and the road surface could act as a wave-guide. Although in [6] the carrier frequency is only 60 GHz, and both the antenna placement and beamwidth differ, the presented measurements therein show that an obstructing vehicle typically causes an 8 dB increased path loss. Due to this experimental contradiction, two different coverage models are proposed in this Letter. The proposal of our Letter is to use a grid-based distribution to model vehicle-to-vehicle (V2V) communications in urban *ad hoc* networks.

B. Contributions

The defining novelty of this Letter is the introduction of a tractable coverage model for mmWave vehicular communications, which:

1) is based on the Manhattan distance to represent the distance between the *typical* transmitter, *typical* receiver and interferers, which is the sum of the vertical and horizontal grid components. Rather than using Euclidean distance, it has been shown in [7] that path loss in an urban environment is closely related to the graph/Manhattan distance and street oriented path loss models for mmWave communications are proposed.

2) proposes a directional antenna gain distribution based on a two-peak truncated normal distribution in order to model vehicular interference more realistically.

3) models that LOS and NLOS separation takes place when the *typical* transmitter-receiver distance is larger than the inverse of density of vehicles per line, λ^{-1}, as a first case, hereafter referred to as *LOS-NLOS*.

4) models LOS and NLOS links for vehicular communications based upon a grid-based distribution, where vehicles on the same line have LOS communications links and line-to-line communications are defined by NLOS links, as a second case, hereafter referred to *LOS-always*. In this way, the linear clustering of vehicles and extreme blockage effect of surrounding buildings are modelled more realistically.

5) therefore, allows for a comparison of the *LOS-NLOS* and *LOS-always* model.

All authors are with WMG, University of Warwick, Coventry CV4 7AL, U.K. (e-mail: m.ozpolat@warwick.ac.uk; e.kampert@warwick.ac.uk; paul.jennings@warwick.ac.uk; m.higgins@warwick.ac.uk).

II. Blockage and Antenna Models

In our model, the blockage of mmWave V2V communications depends on the relative position of the *typical* transmitter, *typical* receiver and interferers on a grid. In the *LOS-NLOS* case, a transition from a LOS to an NLOS link takes place at the position of the nearest obstructing vehicle with respect to the *typical* receiver, i.e. LOS-interference is assumed when the distance between *typical* receiver and interferer is equal or shorter than λ^{-1}m, as shown in Eq. 1, C_1. Alternatively, Eq. 1, C_2 represents the path loss model when the communications link between either the *typical* transmitter and the *typical* receiver, or the interferer and the *typical* receiver is subject to LOS fading when both are positioned on the same grid line. For both cases, when one is positioned on a vertical grid line and the other on a horizontal grid line, the communications link is subject to NLOS fading. When both are located on parallel streets, it is defined that communication is not possible and that interference is negligible.

$$L(r,\lambda) = \begin{cases} C_1 \begin{cases} Ar^{-\alpha_L} & \text{if } \ r \le \lambda^{-1} \\ Ar^{-\alpha_N} & \text{otherwise} \end{cases} \\ C_2 \begin{cases} Ar^{-\alpha_L} & \text{if nodes are on the same road} \\ Ar^{-\alpha_N} & \text{otherwise} \end{cases} \end{cases} \tag{1}$$

with path loss function $L(r,\lambda)$, Manhattan distance between any node r, and path loss intercept A, modelled as $(4\pi f_c/c)^{-2}$ with carrier frequency f_c and speed of light c. The vehicles on a single line form a homogeneous Poisson Point Process (PPP), with a Poisson-distributed number of nodes and a uniform distribution of nodes on the line. The origin is defined as the *typical* receiver location, and related changes of the probability model are prevented by using Slivnyak's theorem and PPP. A clear illustration of the relative positions of *typical* transmitter-receiver and interferers in the proposed blockage model, and the corresponding fading relationships are presented in Fig. 1. Since directional beamforming is frequently proposed to compensate for the high path loss in mmWave communications [8], we define the main lobe antenna gain G and side lobe antenna gain $0 \le g_< \ll 1$ as

$$G_o = \begin{cases} G = \frac{2\pi(2\pi-\phi)g_<}{\phi} & \text{if } \ |\beta| \le \phi/2 \\ g_< & \text{otherwise} \end{cases} \tag{2}$$

with half-power beam width ϕ and beam alignment error β between transmitter and receiver in angular degrees. Hence, the density of interferers is thinned with the probabilities represented by the beam alignment probabilities p_{GG} and p_{gg}, that are bounded by β, which we define as the random variable distributed two-peak truncated normal distribution

$$p_{GG} = \frac{1}{2}\int_{-\frac{\phi}{2}}^{\frac{\phi}{2}} \frac{\frac{1}{\sqrt{2\pi}} e^{\frac{-\theta^2}{2\sigma^2}}}{\frac{\sigma}{2}\left(erf\left(\frac{\pi/2}{\sqrt{2}\sigma}\right) - erf\left(\frac{-\pi/2}{\sqrt{2}\sigma}\right)\right)} d\theta \tag{3}$$

in which θ is the azimuth. Because the most common vehicular communications are with a vehicle at the front or the back of the *typical* transmitter, p_{GG} is the best described with maximum probabilities at 0° and 180°. Thus, we combine truncated normal distributions with zero-mean and π-mean and a standard deviation σ, and normalize the result by dividing by 2. p_{gg} is then defined as $1-p_{GG}$. For simplicity, the effects of mobility, road curvature and undulation on p_{GG} are neglected.

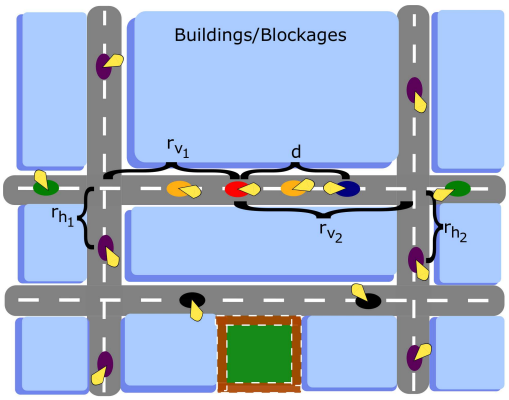

Fig. 1. Graphical representation of the proposed blockage model with the vehicles PPP distributed on each road. The *typical* receiver and transmitter are depicted as red and blue dots, and the NLOS and neglected interferers as purple and black dots, respectively. For the *LOS-NLOS* case, the orange and green dots are LOS and NLOS interferers,respectively, whereas for the *LOS-always* case both orange and green dots are LOS interferers.

III. Coverage Analysis

The definition of the signal-to-interference-plus-noise-ratio (SINR) is presented in Eq. 4 with transmitter power P_t, small scale fading random variable between *typical* transmitter and receiver h_0, distance between *typical* transmitter and receiver d and path loss exponentials for LOS links α_L, distance r, small-scale fading random variable for interferers h_i, path loss exponentials for NLOS links α_N and noise power N_0. $\Phi_{\text{LOS+NLOS}}/\{z\}$ is the group of all interferers, excluding the *typical* transmitter at some position z. The beams of the *typical* transmitter and receiver are defined to be perfectly aligned.

$$\text{SINR} = \frac{P_t G G h_o L(d,\lambda)}{\sum_{i\epsilon\Phi_{\text{LOS+NLOS}}/\{z\}} P_t G_o G_o h_i L(r,\lambda) + N_0} \tag{4}$$

The coverage probability is the likelihood that the received SINR is greater than a specified threshold T. For simplicity, all interference related terms are represented by I_Φ.

$$P_c = 1 - \mathbb{P}\left(h_o < \frac{TL(d,\lambda)}{P_t G G}(I_\Phi + N_0)\right) \tag{5}$$

In our model, small-scale fading is defined to be Nakagami fading, which implements a gamma distributed random variable as it is regarded as the mathematically most appropriate small-scale fading model for mmWave [9]. Alzer's lemma [10] is used in order to calculate the probability term in (5), which states that when $h_0 \sim \Gamma(m, 1/m)$ for an integer m, the probability term is tightly bounded with

$$[1-e^{-az}]^m < \mathbb{P}(h_0 < z), \qquad a = m(m!)^{-1/m} \tag{6}$$

$$P_c < \mathbb{E}_\Phi\left(1 - \left(1 - e^{\frac{-aTL(d,\lambda)}{P_t G G}(N_0+I_\Phi)}\right)^m\right) \tag{7}$$

$$P_c \overset{(a)}{<} \sum_{n=1}^{m} \binom{m}{n} (-1)^{n+1} \mathbb{E}_\Phi\left(e^{\frac{-anTL(d,\lambda)}{P_t G G}(N_0+I_\Phi)}\right) \tag{8}$$

$$P_c \overset{(b)}{<} \sum_{n=1}^{m} \binom{m}{n} (-1)^{n+1} \underbrace{\mathbb{E}_{I_H}\left(e^{\frac{-anTL(d,\lambda)}{P_t GG} I_H}\right)}_{\text{Own Road and } L_H} \underbrace{\mathbb{E}_{V_1}\left(e^{\frac{-anTL(d,\lambda)}{P_t GG} I_{V_1}}\right)}_{\text{Left Vertical Road and } L_{V_1}} \underbrace{\mathbb{E}_{V_2}\left(e^{\frac{-anTL(d,\lambda)}{P_t GG} I_{V_2}}\right)}_{\text{Right Vertical Road and } L_{V_2}} \underbrace{\left(e^{\frac{-anTL(d,\lambda)}{P_t GG} N_0}\right)}_{\text{Noise Term}} \tag{9}$$

$$L_H = \underbrace{\mathbb{E}_{I_H}\left(\prod_{\Phi_H} \mathbb{E}_{h_i}\left(e^{-snP_t GGL(r,\lambda)}\right)\right)}_{\text{Main-Main Lobe Alignment Interference}} \underbrace{\mathbb{E}_{I_H}\left(\prod_{\Phi_H} \mathbb{E}_{h_i}\left(e^{-snP_t ggL(r,\lambda)}\right)\right)}_{\text{Side-Side Lobe Alignment Interference}} \overset{(c)}{=} \prod_{i \epsilon G_{C_i}} \mathbb{E}_{I_H}\left(\prod_{\Phi_H}\left(1 + \frac{snP_t G_i G_i L(r,\lambda)}{m}\right)^{-m}\right) \tag{10}$$

Equation (7) is then obtained by using the expected value operation. In (8), (a) is the binomial expansion of terms in the expected value, and (b) in (9) is extending the terms in the expected value for each path, i.e. the horizontal and vertical roads at both sides of the *typical* receiver. Equation (10) is the Laplace transform of the interference from nodes on the horizontal road, and distributes the expected values for each antenna gain case and small-scale fading random variables, with $s = \frac{aT}{P_t GGL(d,\lambda)}$. For simplicity, the product operator is included for each antenna gain case, represented by $G_{C_i} \epsilon \{GG, p_{GG}; gg, p_{gg}\}$. Then, (c) in (10) is the Moment Generating Function of the gamma random variable.

$$L_H \overset{(d)}{=} \prod_{i \epsilon G_{C_i}} e^{-2p_i\lambda_t\left(\int_R\left(1-\left(1+\frac{snP_t G_i L(r}{m}\right)^{-m}\right)d_{r_h}\right)} \tag{11}$$

The (d) in (11) is the Probability Generating Functional (PGFL) of PPP.

$$L_{H_{C_1}} \overset{(e)}{=} \prod_{i \epsilon G_{C_i}} e^{2p_i\lambda_t\left(Q(r_h;\alpha_L,r_{min},\lambda^{-1})+Q(r_h;\alpha_N,\lambda^{-1},r_{max})\right)} \tag{12}$$

$$L_{H_{C_2}} = \prod_{i \epsilon G_{C_i}} e^{2p_i\lambda_t\left(Q(r_h;\alpha_L,r_{min},r_{max})\right)} \tag{13}$$

$$L_{V_{1_{C_1,C_2}}} = \prod_{i \epsilon G_{C_i}} e^{2p_i\lambda_t\left(Q(r_{h_1}+r_{v_1};\alpha_N,r_{min},r_{max})\right)} \tag{14}$$

$$L_{V_{2_{C_1,C_2}}} = \prod_{i \epsilon G_{C_i}} e^{2p_i\lambda_t\left(Q(r_{h_2}+r_{v_2};\alpha_N,r_{min},r_{max})\right)} \tag{15}$$

The (e) in (12) is the integration of the binomial expansion and following some algebra, with r_{h_1} and r_{h_2} representing the horizontal random variable distances between the *typical* receiver and the vertical roads at both sides, and r_{v_1} and r_{v_2} representing the vertical fixed distances between NLOS interferers and the road on which the *typical* receiver is located, as visualized in Fig. 1. The r_{min} and r_{max} are the integration limits representing the minimum and maximum communications distances, which we define as 0.1 m and 250 m, respectively. Thermal noise and bandwidth are −174 dBm/Hz and 500 MHz for all results. $L_{H_{C_1}}$ and $L_{H_{C_2}}$ are Laplace transforms for horizontal roads for the *LOS-NLOS* and *LOS-always* case, respectively. λ_t is the density of active transmitters, and is defined to be half of λ, as equal numbers of transmitters and receivers are expected.

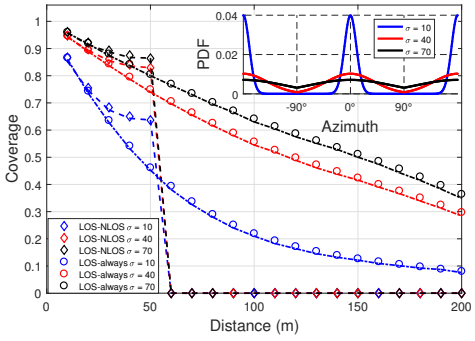

Fig. 2. Dependence of the coverage probability on the distance between *typical* transmitter and receiver for various σ, with markers and lines representing the results from mathematical models and simulations, respectively. Parameters used: $T = 5$ dB, $\lambda_t = 0.01$, $\lambda = 0.02$, $P_t = 1$, $m = 3$, $r_{v_1} = 80$ m, $r_{v_2} = 20$ m, $\phi = \pi/6$, $g_< = 0.1$, $f_c = 60$ GHz, $\alpha_L = 2.7$ and $\alpha_N = 5.4$. Inset: Probability Density Function of the azimuth for various σ.

$L_{V_{1_{C_1,C_2}}}$ and $L_{V_{2_{C_1,C_2}}}$ are Laplace transforms of vertical roads for both cases, with $Q(r;\alpha,r_1,r_2)$ defined as

$$Q(r;\alpha,r_1,r_2) = r\left({}_2F_1\left(\frac{-1}{\alpha}, m; \frac{\alpha-1}{\alpha}; \frac{-snP_t G_i A r^{-\alpha}}{m}\right) - 1\right)\Bigg|_{r_1}^{r_2} \tag{16}$$

The final equation for *LOS-NLOS* coverage analysis is obtained after insertion of (12), (14) and (15) in (9). Similarly, the final equation for *LOS-always* is obtained after insertion of (13), (14) and (15) in (9).

IV. Discussion

A comparison of the obtained analytical equation with Monte Carlo simulations is shown in Fig. 2, 3, 4, displaying a good match between both methods with a mean squared error smaller than 10^{-4}, and providing additional insight in the coverage of mmWave vehicular communications. The simulations are carried out by distributing random nodes on grid-lines and calculating the SINR for each case more than 10^6 times. The limit of the simulation varies between [−250 m 250 m] for all roads.

The results in Fig. 2 represent dense traffic with an interferer vehicle at every 100 m, and display the d-dependence of both the analytical models and the Monte Carlo simulations for various σ. The Probability Density Functions of the azimuthal angle for three chosen σ values is displayed in the inset.

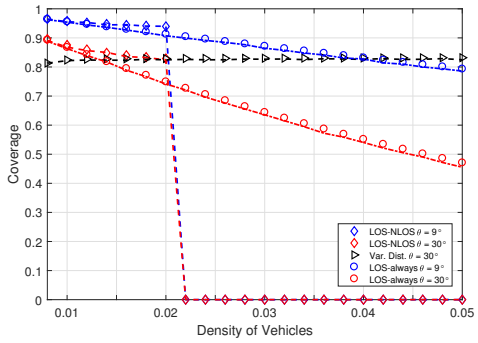

Fig. 3. Dependence of the coverage probability on the density of vehicles for two beam widths with markers and lines representing the results from mathematical models and simulations, respectively. Parameters used: $T = 5\,\text{dB}$, $P_t = 1$, $m = 3$, $d = 50\,\text{m}$, $r_{v_1} = 80\,\text{m}$, $r_{v_2} = 20\,\text{m}$, $g_{\lessdot} = 0.1$, $\sigma = 40$, $f_c = 60\,\text{GHz}$, $\alpha_L = 2.7$ and $\alpha_N = 5.4$.

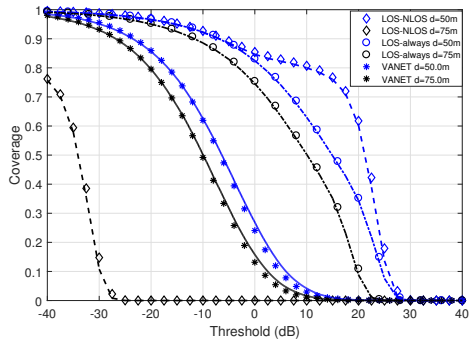

Fig. 4. Dependence of the coverage probability on the SINR threshold for various distances with markers and lines representing the results from mathematical models and simulations. Parameters used: $\lambda_t = 0.01$, $\lambda = 0.02$, $P_t = 1$, $m = 3$, $r_{v_1} = 80\,\text{m}$, $r_{v_2} = 20\,\text{m}$, $\phi = \pi/6$, $g_{\lessdot} = 0.1$, $\sigma = 40$ and $f_c = 60\,\text{GHz}$. Path loss exponentials for mmWave and VANET are $\alpha_L = 2.7$, $\alpha_N = 5.4$, respectively $\alpha_L = 2$, $\alpha_N = 3$.

The steep decrease of the *LOS-NLOS* results for distances larger than 50 m is due to the transition from LOS to NLOS communications at λ^{-1}, after which the coverage rapidly approaches zero. The *LOS-always* results display a gradually decreasing coverage with distance, with the smallest coverage obtained when the largest σ is used for p_{GG} in Eq. 3. In addition, for all cases it is apparent, that interferences from vertical roads only have a limited effect on the coverage, with the largest NLOS interference occurring for small r_{v_1} or r_{v_2}, and the smallest interference occurring when the *typical* receiver is located at equal distances to both vertical roads. As expected, it is evident that for $d \leq \lambda^{-1}$ the *LOS-NLOS* case outperforms the *LOS-always* case for all d, because of the reduced number of LOS-interferers.

Fig. 3 displays the dependence of the coverage probability on the density of interferers for two beam widths ϕ, with the highest coverage being obtained for smallest ϕ. Increasing the beam width results in a reduced gain and a higher interferer beam alignment probability, which both decrease the quality of the communications link. The black markers and line represent the scenario in which the distance between *typical* transmitter and receiver is parametrized as $d = \lambda^{-1}$; when vehicles between the *typical* transmitter and receiver are absent. Hence, in this scenario, a good communications link is always present and slightly *interference-improved*, because the positive effect on the quality of the communications link by the exponentially decreasing path loss with decreasing d overcomes the negative effect of increased interference due to increased λ.

The results in Fig. 4 present the SINR threshold dependence of the coverage probability for various d and for mmWave communications, *LOS-NLOS* and *LOS-always*, and VANET. The latter comparison was made by assigning $m = 1$, lower path loss exponentials α_L and α_N[11], 10 MHz bandwidth, equal lobe alignment probabilities and assigning $G = g_{\lessdot} = 1$ due to omnidirectionality. These results show, that in dense vehicular communications networks, due to large α_L and α_N, mmWave communications significantly outperform lower carrier frequency communications protocols, such as VANET, because of the reduced effect of nearby interferers. NLOS mmWave communications only show poorer coverage performance compared to NLOS VANET communications when $d \geq \lambda^{-1}$.

V. Conclusions

In this Letter, a tractable coverage model for urban mmWave *ad hoc* vehicular networks is presented for two different cases. It is shown that line processes can be used to model vehicular networks, which simplifies the analysis. The mathematical model, verified by Monte Carlo simulations, shows that urban mmWave *ad hoc* vehicular networks could potentially support fully connected traffic, unlike VANET which is more sensitive to an increase in density of transmitters. The analysis shows that by using mmWave, it is possible to fulfill the connectivity needs of a dense traffic scenario, under the condition that communications takes place with vehicles on the same road.

References

[1] J. Choi *et al.*, "Millimeter-wave vehicular communication to support massive automotive sensing," *IEEE Commun. Mag.*, vol. 54, no. 12, pp. 160–167, Dec. 2016.
[2] F. Boccardi *et al.*, "Five disruptive technology directions for 5g," *IEEE Commun. Mag.*, vol. 52, no. 2, pp. 74–80, Feb. 2014.
[3] H. J. Thomas, *et al.*, "An experimental study of the propagation of 55 GHz millimeter waves in an urban mobile radio environment," *IEEE Trans. Veh. Technol.*, vol. 43, no. 1, pp. 140–146, Feb. 1994.
[4] A. Tassi *et al.*, "Modeling and design of millimeter-wave networks for highway vehicular communication," *IEEE Trans. Veh. Technol.*, vol. 66, no. 12, pp. 10 676–10 691, Dec. 2017.
[5] R. Schneider *et al.*, "Impact of road surfaces on millimeter-wave propagation," *IEEE Trans. Veh. Technol.*, vol. 49, no. 4, pp. 1314–1320, July 2000.
[6] A. Yamamoto *et al.*, "Path-loss prediction models for intervehicle communication at 60 ghz," *IEEE Trans. Veh. Technol.*, vol. 57, no. 1, pp. 65–78, Jan. 2008.
[7] A. Karttunen *et al.*, "Spatially consistent street-by-street path loss model for 28-ghz channels in micro cell urban environments," *IEEE Trans. Wireless Commun.*, vol. 16, no. 11, pp. 7538–7550, Nov. 2017.
[8] J. Wildman *et al.*, "On the joint impact of beamwidth and orientation error on throughput in directional wireless poisson networks," *IEEE Trans. Wireless Commun.*, vol. 13, no. 12, pp. 7072–7085, Dec. 2014.
[9] A. Thornburg *et al.*, "Performance Analysis of Outdoor mmWave Adhoc Networks," *IEEE Trans. Signal Process.*, vol. 64, no. 15, pp. 4065–4079, Aug. 2016.
[10] H. Alzer, "On some inequalities for the incomplete gamma function," *Math. Comput.*, vol. 66, no. 218, pp. 771–778, Apr. 1997.
[11] H. Fernandez *et al.*, "Path loss characterization in vehicular environments under los and nlos conditions at 5.9 ghz," in *The 8th European Conf. Antennas and Propagation (EuCAP)*, The Hague, Netherlands, 2014, pp. 3044–3048.